Bull. Soc. R. Sci. Liège, 2024, **93**(2), 358–369 *Peer-reviewed conference paper*
doi:10.25518/0037-9565.11717

Understanding the Magnetic Activity of M Dwarfs: Optical and Near-Infrared Spectroscopic Studies

Diya RAM[1,*], Soumen MONDAL[1,*], Samrat GHOSH[1], Santosh JOSHI[2], Dusmanta PATRA[1] and Rajib KUMBHAKAR[1]

[1] S. N. Bose National Centre for Basic Sciences, Kolkata 700106, India
[2] Aryabhatta Research Institute of Observational Sciences, Nainital 263002, India
[*] Corresponding authors: ramdiya1996@gmail.com; soumen.mondal@bose.res.in

Paper presented at the 3rd BINA Workshop on "Scientific Potential of the Indo-Belgian Cooperation", held at the Graphic Era Hill University, Bhimtal (India), 22nd–24th March 2023.

Abstract

We present here preliminary results of stellar activities on three active M dwarfs having strong magnetic fields using optical and Near-Infrared (NIR) (0.38 μm–2.5 μm) spectroscopic observational data using HFOSC on the 2-m HCT and TANSPEC on the 3.6-m DOT. The sample includes new observations of AD Leo, EV Lac, and Stkm2-809 M dwarfs, including published literature values of 89 M dwarfs. To understand the magnetic field activity on those dwarfs, we used the equivalent widths of spectral features Ca IRT triplet (0.850 μm, 0.854 μm, 0.866 μm), which are generally chromospheric and coronal indicators in M dwarfs, and investigate the correlation between those line strengths with Rossby number, which is defined as the ratio of rotation period (P_{rot}) to convective turnover time ($\tau_{\rm conv}$). We find a strong correlation between the equivalent widths of Ca IRT b and Ca IRT c and Rossby number (R_0). The correlation shows an increasing trend of equivalent widths of those lines with decreasing R_0, and saturation of the equivalent widths of those at lower $R_0 \leq 0.1$. To estimate R_0, we estimate the rotation periods of three observed M dwarfs in our sample from TESS data, and in the case of other M dwarfs, we used the literature values. Interestingly, in TESS light curves of AD Leo, EV Lac, and Stkm2-809 M dwarfs, we find several flare events. We estimated the bolometric flared energy in a range of 10^{34} to 10^{37} erg, which is in the superflare range (more than 10^{32} erg). We estimate the highest flared energy of 1.22×10^{37} erg for EV Lac in TESS sector 57. To produce such kind of high superflare event, we have estimated the required magnetic field strength of 10.53 kG, which will have an impact on the life habitability of planets around such M dwarfs.

Keywords: TESS - M dwarfs - Flare - Rossby number

1. Introduction

M dwarfs are the lowest-mass hydrogen-burning stars, which are found at the bottom of the main sequence in the H–R diagram, the most numerous stars in our Galaxy, about 40% in stellar

mass (Kirkpatrick et al., 2012). These stars possess masses of 0.08–0.6 $M_{\odot}$ and have $T_{\rm eff}$ of 2500–4000 K (Pecaut and Mamajek, 2013). M dwarfs exhibit conspicuous evidence of surface activity, e.g., flares, photometric rotational variability, enhanced chromospheric and coronal emission in X-rays, UV, optical/IR, and radio (Hawley et al., 2014; Newton et al., 2016). An interesting feature of the magnetic activity signature is the saturation with the Rossby number, R_0, which can be defined as the ratio of rotation period, $P_{\rm rot}$, and convective turnover time, $\tau_{\rm conv}$. For $R_0 \geq 0.1$, stars show a log-linear relationship between the strength of magnetic indicators and R_0; however, for $R_0 \leq 0.1$, the relationship is flat (Muirhead et al., 2020). The saturation of R_0 is observed in Sun-like stars (Pallavicini et al., 1981), and similar behavior is also observed for M dwarfs of the fully convective boundary (Newton et al., 2017).

Another exciting feature of stellar activity is the stellar flare, which occurs due to the magnetic reconnection in the stellar atmosphere accelerating charged particles into the photosphere, heating the plasma, and releasing energy across the electromagnetic spectrum (Howard, 2022). Low-mass stars can remain active for 10 Gyr (France et al., 2020) and frequently emit superflares 10 to 1000 times larger than flares from our Sun (Howard et al., 2018). Such kind of superflares may affect the habitability of terrestrial planets orbiting in the liquid-water habitable zones of these stars (Howard, 2022).

In this paper, we present preliminary results of stellar activities on three active M dwarfs using optical and Near-IR (0.38–2.5 μm) spectroscopic observational data. The sample in this study includes new observations of AD Leo, EV Lac, and Stkm2-809 M dwarfs, including 89 M dwarfs taken from the literature (Khata et al., 2021). We used the equivalent widths of spectral features Ca IRT b (0.854 μm) and Ca IRT c (0.866 μm), which are generally chromospheric and coronal indicators in M dwarfs. To understand the magnetic field activity on those dwarfs, we investigate the correlation between those line strengths of Ca IRT and R_0. We have also analyzed the flared light curves of those dwarfs to estimate the flared energy and estimate the magnetic fields to produce such kinds of flared events. Section 2 describes the spectroscopic and photometric observations and data analysis. In Section 3, we discuss the preliminary results of the above-mentioned studies. Finally, we have summarized our results in Section 4.

2. Observations and Data Reductions

2.1. Photometry

TESS (Ricker et al., 2014), which was launched in April 2018, has immensely magnified the number of planets for detailed characterization, over 5000 extrasolar TESS Objects of Interest (TOI, (Guerrero et al., 2021)) have so far been detected. TESS searches the entire sky for both transiting exoplanets and astrophysical variability in a tiling-based approach. The sky is split into $24^{\circ} \times 96^{\circ}$ sectors, each sector is observed for 27 d at a time with four onboard 10.5 cm telescopes in a red (600–1000 nm) bandpass. First, we used the lightkurve package (Lightkurve Collaboration et al., 2018) to download the TESS light curves of our targets such as AD Leo for sector 48; EV Lac for sectors 7, 56, 57; Stkm2-809 for sectors 22, 48 from Mikulski Archive for Space Telescopes (MAST archive). Then, the Science Processing Operations Center (SPOC)

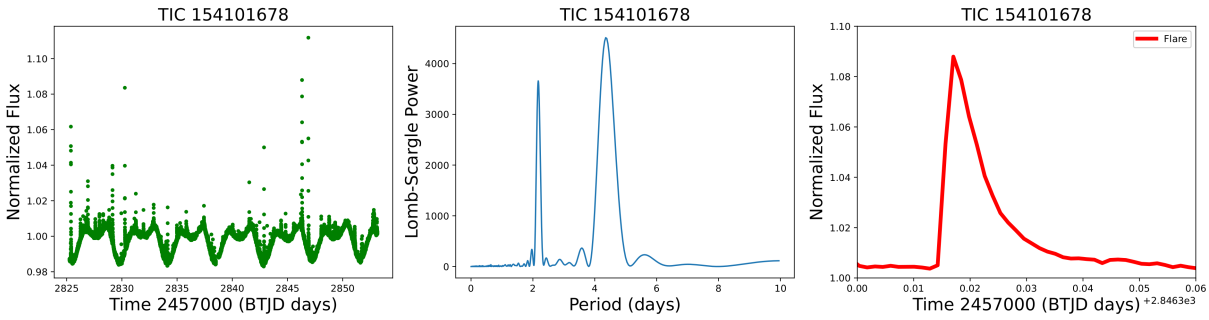

Figure 1: (left) An example of the TESS light curve. (middle) The Lomb-Scargle Periodogram of that light curve. (right) The flare event of EV Lac in Sector 56.

pipeline (Jenkins et al., 2016) extracts the data (see Fig. 1).

2.2. Spectroscopy

The Optical spectra of three M dwarfs are obtained using medium resolution (≈1200) Hanle Faint Object Spectrograph and Camera (HFOSC) on the 2.0-m Himalayan *Chandra* Telescope (HCT) located at Hanle, India. The spectra (350–900 nm) are taken with grism 7 and grism 8. The optical and Near-Infrared (NIR) spectra are taken with cross-disperser mode with a wavelength range of 0.55–2.5 μm with slit width 1 arcsec using medium resolution (≈ 2750) TIFR-ARIES Near Infrared Spectrometer (TANSPEC) on the 3.6-m Devasthal Optical Telescope (DOT) located at Devasthal, India during several observing nights over 2021 to 2023. The TANSPEC data have been reduced with the TANSPEC pipeline (Ghosh et al., 2023), and are cross-checked with the IRAF reduction (see Fig. 2). We measured the equivalent width (*EW*) of spectral features like Ca IRT b (0.854 μm) and Ca IRT c (0.866 μm) using the standard equation

$$EW_\lambda = \int_{\lambda_1}^{\lambda_2} [1 - F(\lambda)/F_c(\lambda)]\, d\lambda,$$

where $F(\lambda)$ represents the flux across the wavelength range of the line (λ_2–λ_1), and $F_c(\lambda)$ stands for the estimated continuum flux on either side of the absorption line. The *EW* is measured using the *Python*-based package SPECUTILS for our observed samples.

3. Results and Discussion

3.1. Rotation periods

Periodic variation in light curves of low mass M-dwarfs can be observed due to rotation of star. This is due to presence of large star-spot which is cooler than its surroundings, rotating in and out of view (McQuillan et al., 2013). Flares originate in active regions of Sun where spots found. Therefore, due to the presence of spots, large variations in brightness in the light curves of M-dwarfs are observed (Doyle et al., 2019). To search for a significant periodic signal, we used the Lomb-Scargle (LS) periodogram package from NASA Exoplanet Archive Periodogram

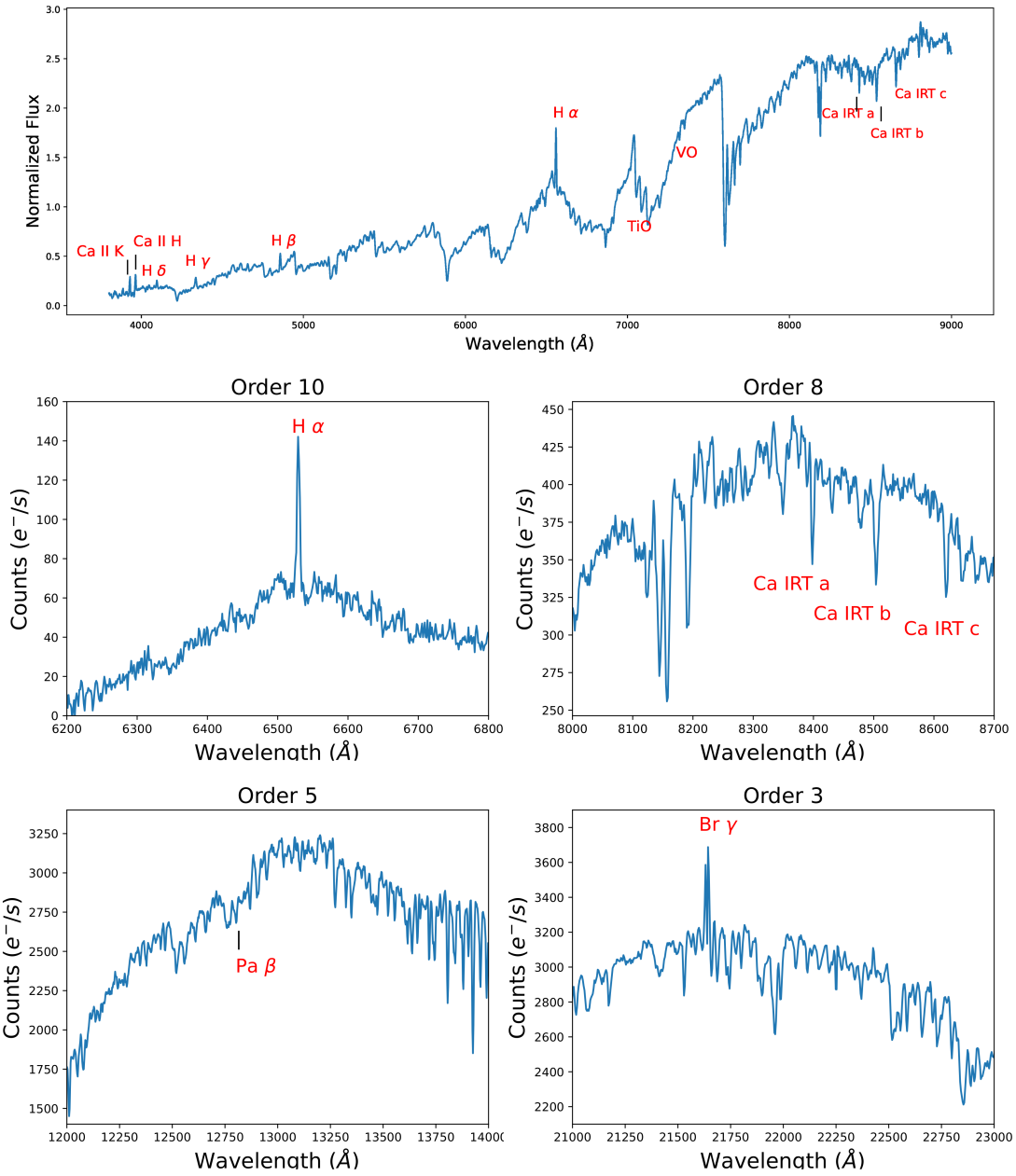

Figure 2: The optical spectra of AD Leo taken from the 2-m HCT (top), optical spectra of Stkm2-809 from 3.6-m DOT (middle) and Near-IR spectra of Stkm2-809 from 3.6-m DOT (bottom) are shown here. Chromospheric indicator's spectral features are marked on those spectra.

Table 1: Results for the rotation periods

Object	TIC	Sector	Period		Reference
			This work (d)	Literature (d)	
AD Leo	91531305	48	2.20	2.23	Lafarga et al. (2021)
EV Lac	154101678	56	4.35	4.38	Wright et al. (2011)
Stkm2-809	416538839	48	0.72	0.73	Ribas et al. (2023)

Table 2: Estimation of magnetic field of flared event

Object	TIC	Sector	Highest Flare Energy (erg)	Magnetic Field Flare Event (kG)
AD Leo	91531305	48	2.08×10^{36}	2.48
EV Lac	154101678	57	1.22×10^{37}	10.53
Stkm2-809	416538839	48	5.23×10^{35}	0.85

Service to find the significant periodic signal. The LS periodogram (Lomb, 1976; Scargle, 1982) method uses a Fourier power spectrum estimator to find out significant periodicity, and it can deal with the observed sparse data sets. In Table 1, the estimated rotation periods of three M dwarfs in this work are listed, which are fairly close to previously estimated literature values.

3.2. Stellar flares

First, we estimated the equivalent duration (ED) of the flare, which is the equivalent time during which a substellar object (in its quiescent state) would have emitted the same amount of energy as the flare emitted, which is measured as flare energy (Gershberg, 1972):

$$ED = \int F_{\rm flare}(t)/F_0\, dt,$$

where F_{flare} is the integrated flare flux and F_0 the median quiescent flux. To estimate ED, we implemented the open-source *Python* software ALTAIPONY which is used to calculate the energy of flares. Following the method from Shibayama et al. (2013), we calculate the flare energy from the stellar luminosity and the best-fitting flare profile. Finally, we arrive at the expression for the bolometric energy of the flare, given as

$$E_{\rm flare} = \int L'_{\rm flare}(t)\, dt,$$

where $L'_{\rm flare}$ is the bolometric flare luminosity. We estimated the flare energy of those M-dwarfs, having E_{flare} in a range of 10^{34} to 10^{37} erg, which is in the superflare range (more than 10^{32} erg), and listed in Table 2. Interestingly, we measured the highest flare of energy 1.22×10^{37} erg in TESS sector 57 for EV Lac.

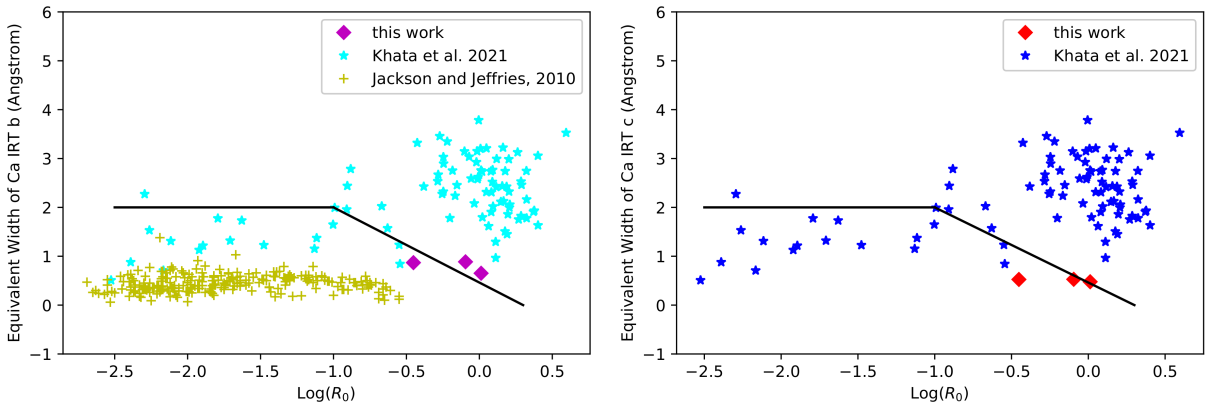

Figure 3: Equivalent width vs Rossby number R_0 for Ca IRT b (0.854 μm; left) and Ca IRT c (0.866 μm; right) lines.

3.3. Estimation of magnetic field with flared energy

According to Aulanier et al. (2013) and Paudel et al. (2018), considering the flare events are similar to solar flares, we can roughly estimate the maximum strength of the magnetic field ($B_z^{\rm max}$) to produce such superflares following the relation

$$E_{\rm flare} = 0.5 \times 10^{32} \times \left(\frac{B_Z^{\rm max}}{1000\,{\rm G}}\right)^2 \times \left(\frac{L^{\rm bipole}}{50\,{\rm Mm}}\right)^3 \ {\rm erg},$$

where $E_{\rm flare}$ is the bolometric flare energy and $L^{\rm bipole}$ the linear separation between a pair of magnetic poles on the surface of the objects, which is taken to be $L^{\rm bipole} = \pi R$, with R being the radius of the star. In Table 2, we have estimated the magnetic field of flared events in M dwarfs. To produce the highest flare energy 1.22×10^{37} erg like superflare event in EV Lac in TESS sector 57, we have estimated the required magnetic field strength, which is coming out in order of 10.53 kG.

3.4. Correlation of chromospheric line indicators with Rossby number

The Rossby number (R_0) is defined as the ratio of rotation period ($P_{\rm rot}$) to convective turnover time ($\tau_{\rm conv}$): $R_0 = P_{\rm rot}/\tau_{\rm conv}$. To estimate R_0, we have calculated $\tau_{\rm conv}$ from the relation given by Wright et al. (2011) using masses. Masses of all dwarfs are taken from Stassun et al. (2019) by using the mass-M_K relation from Mann et al. (2019). Because of parallax and M_K uncertaintities, the final uncertainties on masses are usually 3–4%. The rotation periods of AD Leo, EV Lac and Stkm2-809 are measured in this work from the TESS light curves, and those of the remaining 89 dwarfs are taken from Astudillo-Defru et al. (2017) with error bars calculated by propagation. The uncertainty in measuring R_0 are due to uncertainties in the estimations of mass and $\tau_{\rm conv}$. EWs of Ca IRT b (0.854 μm) and Ca IRT c (0.866 μm) of three M dwarfs are measured in this work, and those of 89 M dwarfs are taken from Khata et al. (2021). In Fig. 3, we preliminarily report the variation of EW of Ca IRT b and Ca IRT c with R_0. For comparison, we have also taken data for another 237 M dwarfs from Jackson and Jeffries (2010). We find that For $R_0 \geq 0.1$, it shows a log-linear relationship between the strength

of magnetic indicators and R_0. However, for $R_0 \leq 0.1$, the relationship is flat, indicating that the magnetic fields in the photosphere itself are saturated (Reiners et al., 2009).

4. Summary and Conclusions

In this work, we present here preliminary results of stellar activities on three active M dwarfs having strong magnetic fields using optical and Near-Infrared (NIR) (0.38–2.5 μm) spectroscopic observational data. To understand the magnetic field activity on those dwarfs, we used the correlation between equivalent widths of spectral features Ca IRT b and Ca IRT c with Rossby number, which shows a log-linear relationship for $R_0 \geq 0.1$, while for $R_0 \leq 0.1$, the relationship is saturated. The rotation periods of our sample are measured using the TESS data. We measured the flare energy of three M-dwarfs, having the bolometric flared energy in a range of 10^{34} to 10^{37} erg, which are in the superflare range (more than 10^{32} erg). We have estimated the required magnetic field strength for such flare events, which is in the range of 0.85 to 10.5 kG.

Acknowledgments

We would like to thank the referee, for him/her valuable comments, suggestions on our paper which helped to improve the manuscript. This research work is financially supported by S. N. Bose National Centre for Basic Sciences under the Department of Science and Technology, Govt. of India. This study uses TESS mission data from the Space Telescope Science Institute (STScI). The NASA Explorer Program provides funding for the TESS mission. STScI is operated by the Association of Universities for Research in Astronomy, Inc., under NASA contract NAS 5-26555. The authors acknowledge the observing facilities, time allocation committee members, and the staff of HCT and DOT, operated by IIA, Bangalore, and ARIES, Nainital.

Further Information

Authors' ORCID identifiers

0009-0008-7884-3741 (Diya RAM)
0000-0003-1457-0541 (Soumen MONDAL)
0000-0003-3354-850X (Samrat GHOSH)
0009-0007-1545-854X (Santosh JOSHI)
0000-0002-7018-4349 (Dusmanta PATRA)
0000-0001-7277-2577 (Rajib KUMBHAKAR)

Author contributions

DR carried out the light curve analyses as well as spectroscopic data analysis. The text was written by DR and SM. All authors contributed to the discussion and interpretation of the results and commented on the written draft of the paper.

Conflicts of interest

The authors declare no conflict of interest.

References

Astudillo-Defru, N., Delfosse, X., Bonfils, X., Forveille, T., Lovis, C. and Rameau, J. (2017) Magnetic activity in the HARPS M dwarf sample. The rotation-activity relationship for very low-mass stars through $R'_{\rm HK}$. A&A, 600, A13. https://doi.org/10.1051/0004-6361/201527078.

Aulanier, G., Démoulin, P., Schrijver, C. J., Janvier, M., Pariat, E. and Schmieder, B. (2013) The standard flare model in three dimensions. II. Upper limit on solar flare energy. A&A, 549, A66. https://doi.org/10.1051/0004-6361/201220406.

Doyle, L., Ramsay, G., Doyle, J. G. and Wu, K. (2019) Probing the origin of stellar flares on M dwarfs using TESS data sectors 1–3. MNRAS, 489(1), 437–445. https://doi.org/10.1093/mnras/stz2205.

France, K., Duvvuri, G., Egan, H., Koskinen, T., Wilson, D. J., Youngblood, A., Froning, C. S., Brown, A., Alvarado-Gómez, J. D., Berta-Thompson, Z. K., Drake, J. J., Garraffo, C., Kaltenegger, L., Kowalski, A. F., Linsky, J. L., Loyd, R. O. P., Mauas, P. J. D., Miguel, Y., Pineda, J. S., Rugheimer, S., Schneider, P. C., Tian, F. and Vieytes, M. (2020) The high-energy radiation environment around a 10 Gyr M dwarf: Habitable at last? AJ, 160(5), 237. https://doi.org/10.3847/1538-3881/abb465.

Gershberg, R. E. (1972) Some results of the cooperative photometric observations of the UV Cet-type flare stars in the years 1967–71. ApSS, 19(1), 75–92. https://doi.org/10.1007/BF00643168.

Ghosh, S., Ninan, J. P., Ojha, D. K. and Sharma, S. (2023) PYTANSPEC: A data reduction package for TANSPEC. JApA, 44(1), 30. https://doi.org/10.1007/s12036-023-09926-y.

Guerrero, N. M., Seager, S., Huang, C. X., Vanderburg, A., Garcia Soto, A., Mireles, I., Hesse, K., Fong, W., Glidden, A., Shporer, A., Latham, D. W., Collins, K. A., Quinn, S. N., Burt, J., Dragomir, D., Crossfield, I., Vanderspek, R., Fausnaugh, M., Burke, C. J., Ricker, G., Daylan, T., Essack, Z., Günther, M. N., Osborn, H. P., Pepper, J., Rowden, P., Sha, L., Villanueva, J., Steven, Yahalomi, D. A., Yu, L., Ballard, S., Batalha, N. M., Berardo, D., Chontos, A., Dittmann, J. A., Esquerdo, G. A., Mikal-Evans, T., Jayaraman, R., Krishnamurthy, A., Louie, D. R., Mehrle, N., Niraula, P., Rackham, B. V., Rodriguez, J. E., Rowden, S. J. L., Sousa-Silva, C., Watanabe, D., Wong, I., Zhan, Z., Zivanovic, G., Christiansen, J. L., Ciardi, D. R., Swain, M. A., Lund, M. B., Mullally, S. E., Fleming, S. W., Rodriguez, D. R., Boyd, P. T., Quintana, E. V., Barclay, T., Colón, K. D., Rinehart, S. A., Schlieder, J. E., Clampin, M., Jenkins, J. M., Twicken, J. D., Caldwell, D. A., Coughlin, J. L., Henze, C., Lissauer, J. J., Morris, R. L., Rose, M. E., Smith, J. C., Tenenbaum, P., Ting, E. B., Wohler, B., Bakos,

G. Á., Bean, J. L., Berta-Thompson, Z. K., Bieryla, A., Bouma, L. G., Buchhave, L. A., Butler, N., Charbonneau, D., Doty, J. P., Ge, J., Holman, M. J., Howard, A. W., Kaltenegger, L., Kane, S. R., Kjeldsen, H., Kreidberg, L., Lin, D. N. C., Minsky, C., Narita, N., Paegert, M., Pál, A., Palle, E., Sasselov, D. D., Spencer, A., Sozzetti, A., Stassun, K. G., Torres, G., Udry, S. and Winn, J. N. (2021) The TESS Objects of Interest Catalog from the TESS Prime Mission. ApJS, 254(2), 39. https://doi.org/10.3847/1538-4365/abefe1.

Hawley, S. L., Davenport, J. R. A., Kowalski, A. F., Wisniewski, J. P., Hebb, L., Deitrick, R. and Hilton, E. J. (2014) *Kepler* flares. I. Active and inactive M dwarfs. ApJ, 797(2), 121. https://doi.org/10.1088/0004-637X/797/2/121.

Howard, W. S. (2022) The flaring TESS Objects of Interest: flare rates for all two-minute cadence TESS planet candidates. MNRAS, 512(1), L60–L65. https://doi.org/10.1093/mnrasl/slac024.

Howard, W. S., Tilley, M. A., Corbett, H., Youngblood, A., Loyd, R. O. P., Ratzloff, J. K., Law, N. M., Fors, O., del Ser, D., Shkolnik, E. L., Ziegler, C., Goeke, E. E., Pietraallo, A. D. and Haislip, J. (2018) The first naked-eye superflare detected from Proxima Centauri. ApJ, 860(2), L30. https://doi.org/10.3847/2041-8213/aacaf3.

Jackson, R. J. and Jeffries, R. D. (2010) Chromospheric activity among fast-rotating M dwarfs in the open cluster NGC 2516. MNRAS, 407(1), 465–478. https://doi.org/10.1111/j.1365-2966.2010.16917.x.

Jenkins, J. M., Twicken, J. D., McCauliff, S., Campbell, J., Sanderfer, D., Lung, D., Mansouri-Samani, M., Girouard, F., Tenenbaum, P., Klaus, T., Smith, J. C., Caldwell, D. A., Chacon, A. D., Henze, C., Heiges, C., Latham, D. W., Morgan, E., Swade, D., Rinehart, S. and Vanderspek, R. (2016) The TESS science processing operations center. In Software and Cyberinfrastructure for Astronomy IV, edited by Chiozzi, G. and Guzman, J. C., vol. 9913. https://doi.org/10.1117/12.2233418.

Khata, D., Mondal, S., Das, R. and Baug, T. (2021) Estimating $T_{\rm eff}$, radius, and luminosity of M-dwarfs using high-resolution optical and NIR spectral features. MNRAS, 507(2), 1869–1885. https://doi.org/10.1093/mnras/stab2211.

Kirkpatrick, J. D., Gelino, C. R., Cushing, M. C., Mace, G. N., Griffith, R. L., Skrutskie, M. F., Marsh, K. A., Wright, E. L., Eisenhardt, P. R., McLean, I. S., Mainzer, A. K., Burgasser, A. J., Tinney, C. G., Parker, S. and Salter, G. (2012) Further defining spectral type "Y" and exploring the low-mass end of the field brown dwarf mass function. ApJ, 753(2), 156. https://doi.org/10.1088/0004-637X/753/2/156.

Lafarga, M., Ribas, I., Reiners, A., Quirrenbach, A., Amado, P. J., Caballero, J. A., Azzaro, M., Béjar, V. J. S., Cortés-Contreras, M., Dreizler, S., Hatzes, A. P., Henning, T., Jeffers, S. V., Kaminski, A., Kürster, M., Montes, D., Morales, J. C., Oshagh, M., Rodríguez-López, C., Schöfer, P., Schweitzer, A. and Zechmeister, M. (2021) Mapping magnetic activity indicators

across the M dwarf domain. In The Star-Planet Connection, p. 7. https://doi.org/10.5281/zenodo.5592214.

Lightkurve Collaboration, Cardoso, J. V. d. M., Hedges, C., Gully-Santiago, M., Saunders, N., Cody, A. M., Barclay, T., Hall, O., Sagear, S., Turtelboom, E., Zhang, J., Tzanidakis, A., Mighell, K., Coughlin, J., Bell, K., Berta-Thompson, Z., Williams, P., Dotson, J. and Barentsen, G. (2018) Lightkurve: Kepler and TESS time series analysis in Python. Astrophysics Source Code Library, record ascl:1812.013.

Lomb, N. R. (1976) Least-squares frequency analysis of unequally spaced data. ApSS, 39(2), 447–462. https://doi.org/10.1007/BF00648343.

Mann, A. W., Dupuy, T., Kraus, A. L., Gaidos, E., Ansdell, M., Ireland, M., Rizzuto, A. C., Hung, C.-L., Dittmann, J., Factor, S., Feiden, G., Martinez, R. A., Ruíz-Rodríguez, D. and Thao, P. C. (2019) How to constrain your M dwarf. II. The mass-luminosity-metallicity relation from 0.075 to 0.70 solar masses. ApJ, 871(1), 63. https://doi.org/10.3847/1538-4357/aaf3bc.

McQuillan, A., Aigrain, S. and Mazeh, T. (2013) Measuring the rotation period distribution of field M dwarfs with *Kepler*. MNRAS, 432(2), 1203–1216. https://doi.org/10.1093/mnras/stt536.

Muirhead, P. S., Veyette, M. J., Newton, E. R., Theissen, C. A. and Mann, A. W. (2020) Magnetic inflation and stellar mass. V. Intensification and saturation of M-dwarf absorption lines with Rossby number. AJ, 159(2), 52. https://doi.org/10.3847/1538-3881/ab5d3d.

Newton, E. R., Irwin, J., Charbonneau, D., Berlind, P., Calkins, M. L. and Mink, J. (2017) The Hα emission of nearby M dwarfs and its relation to stellar rotation. ApJ, 834(1), 85. https://doi.org/10.3847/1538-4357/834/1/85.

Newton, E. R., Irwin, J., Charbonneau, D., Berta-Thompson, Z. K., Dittmann, J. A. and West, A. A. (2016) The rotation and Galactic kinematics of mid M dwarfs in the solar neighborhood. ApJ, 821(2), 93. https://doi.org/10.3847/0004-637X/821/2/93.

Pallavicini, R., Golub, L., Rosner, R., Vaiana, G. S., Ayres, T. and Linsky, J. L. (1981) Relations among stellar X-ray emission observed from *Einstein*, stellar rotation and bolometric luminosity. ApJ, 248, 279–290. https://doi.org/10.1086/159152.

Paudel, R. R., Gizis, J. E., Mullan, D. J., Schmidt, S. J., Burgasser, A. J., Williams, P. K. G. and Berger, E. (2018) *K2* ultracool dwarfs survey. IV. Monster flares observed on the young brown dwarf CFHT-BD-Tau 4. ApJ, 861(2), 76. https://doi.org/10.3847/1538-4357/aac8e0.

Pecaut, M. J. and Mamajek, E. E. (2013) Intrinsic colors, temperatures, and bolometric corrections of pre-main-sequence stars. ApJS, 208(1), 9. https://doi.org/10.1088/0067-0049/208/1/9.

Reiners, A., Basri, G. and Browning, M. (2009) Evidence for magnetic flux saturation in rapidly rotating M stars. ApJ, 692(1), 538–545. https://doi.org/10.1088/0004-637X/692/1/538.

Ribas, I., Reiners, A., Zechmeister, M., Caballero, J. A., Morales, J. C., Sabotta, S., Baroch, D., Amado, P. J., Quirrenbach, A., Abril, M., Aceituno, J., Anglada-Escudé, G., Azzaro, M., Barrado, D., Béjar, V. J. S., Benítez de Haro, D., Bergond, G., Bluhm, P., Calvo Ortega, R., Cardona Guillén, C., Chaturvedi, P., Cifuentes, C., Colomé, J., Cont, D., Cortés-Contreras, M., Czesla, S., Díez-Alonso, E., Dreizler, S., Duque-Arribas, C., Espinoza, N., Fernández, M., Fuhrmeister, B., Galadí-Enríquez, D., García-López, A., González-Álvarez, E., González Hernández, J. I., Guenther, E. W., de Guindos, E., Hatzes, A. P., Henning, T., Herrero, E., Hintz, D., Huelmo, Á. L., Jeffers, S. V., Johnson, E. N., de Juan, E., Kaminski, A., Kemmer, J., Khaimova, J., Khalafinejad, S., Kossakowski, D., Kürster, M., Labarga, F., Lafarga, M., Lalitha, S., Lampón, M., Lillo-Box, J., Lodieu, N., López González, M. J., López-Puertas, M., Luque, R., Magán, H., Mancini, L., Marfil, E., Martín, E. L., Martín-Ruiz, S., Molaverdikhani, K., Montes, D., Nagel, E., Nortmann, L., Nowak, G., Pallé, E., Passegger, V. M., Pavlov, A., Pedraz, S., Perdelwitz, V., Perger, M., Ramón-Ballesta, A., Reffert, S., Revilla, D., Rodríguez, E., Rodríguez-López, C., Sadegi, S., Sánchez Carrasco, M. Á., Sánchez-López, A., Sanz-Forcada, J., Schäfer, S., Schlecker, M., Schmitt, J. H. M. M., Schöfer, P., Schweitzer, A., Seifert, W., Shan, Y., Skrzypinski, S. L., Solano, E., Stahl, O., Stangret, M., Stock, S., Stürmer, J., Tabernero, H. M., Tal-Or, L., Trifonov, T., Vanaverbeke, S., Yan, F. and Zapatero Osorio, M. R. (2023) The CARMENES search for exoplanets around M dwarfs. Guaranteed time observations Data Release 1 (2016–2020). A&A, 670, A139. https://doi.org/10.1051/0004-6361/202244879.

Ricker, G. R., Winn, J. N., Vanderspek, R., Latham, D. W., Bakos, G. Á., Bean, J. L., Berta-Thompson, Z. K., Brown, T. M., Buchhave, L., Butler, N. R., Butler, R. P., Chaplin, W. J., Charbonneau, D., Christensen-Dalsgaard, J., Clampin, M., Deming, D., Doty, J., De Lee, N., Dressing, C., Dunham, E. W., Endl, M., Fressin, F., Ge, J., Henning, T., Holman, M. J., Howard, A. W., Ida, S., Jenkins, J., Jernigan, G., Johnson, J. A., Kaltenegger, L., Kawai, N., Kjeldsen, H., Laughlin, G., Levine, A. M., Lin, D., Lissauer, J. J., MacQueen, P., Marcy, G., McCullough, P. R., Morton, T. D., Narita, N., Paegert, M., Palle, E., Pepe, F., Pepper, J., Quirrenbach, A., Rinehart, S. A., Sasselov, D., Sato, B., Seager, S., Sozzetti, A., Stassun, K. G., Sullivan, P., Szentgyorgyi, A., Torres, G., Udry, S. and Villasenor, J. (2014) Transiting Exoplanet Survey Satellite (TESS). In Space Telescopes and Instrumentation 2014: Optical, Infrared, and Millimeter Wave, edited by Oschmann, J., Jacobus M., Clampin, M., Fazio, G. G. and MacEwen, H. A., vol. 9143. SPIE. https://doi.org/10.1117/12.2063489.

Scargle, J. D. (1982) Studies in astronomical time series analysis. II. Statistical aspects of spectral analysis of unevenly spaced data. ApJ, 263, 835–853. https://doi.org/10.1086/160554.

Shibayama, T., Maehara, H., Notsu, S., Notsu, Y., Nagao, T., Honda, S., Ishii, T. T., Nogami, D. and Shibata, K. (2013) Superflares on solar-type stars observed with *Kepler*. I. Statistical properties of superflares. ApJS, 209(1), 5. https://doi.org/10.1088/0067-0049/209/1/5.

Stassun, K. G., Oelkers, R. J., Paegert, M., Torres, G., Pepper, J., De Lee, N., Collins, K., Latham, D. W., Muirhead, P. S., Chittidi, J., Rojas-Ayala, B., Fleming, S. W., Rose, M. E., Tenenbaum, P., Ting, E. B., Kane, S. R., Barclay, T., Bean, J. L., Brassuer, C. E., Charbonneau, D., Ge, J., Lissauer, J. J., Mann, A. W., McLean, B., Mullally, S., Narita, N., Plavchan, P., Ricker, G. R., Sasselov, D., Seager, S., Sharma, S., Shiao, B., Sozzetti, A., Stello, D., Vanderspek, R., Wallace, G. and Winn, J. N. (2019) The revised TESS Input Catalog and Candidate Target List. AJ, 158(4), 138. https://doi.org/10.3847/1538-3881/ab3467.

Wright, N. J., Drake, J. J., Mamajek, E. E. and Henry, G. W. (2011) The stellar-activity-rotation relationship and the evolution of stellar dynamos. ApJ, 743(1), 48. https://doi.org/10.1088/0004-637X/743/1/48.